ROTATIONAL MOTION OF TOWER CRANE - DYNAMIC ANALYSIS AND REGULATION USING SCHEMATIC MODELING

Prof.dr. Doçi Ilir, Prof.ass. Lajqi Shpetim*
Faculty of Mechanical Engineering –University of Prishtina, Kosovo (ilir.doci@uni-pr.edu)
*Corresponding author (shpetim.lajqi@uni-pr.edu)

Abstract: *This paper deals with dynamic analysis of particular type Construction Cranes known as tower crane during rotational motion of its jib. Methodology of analysis consists of Schematic Design of model, which implements schemes with block diagrams to analyze cranes and their parts during particular work cycle. This procedure consists of crane model development of interconnected elements that represents crane parts, 3-D visualization and simulation of motion. Analysis will be carried out through simulations, and solution of Euler differential equations of second order gained from schematic model. Dynamic parameters investigated are: acceleration, angular velocity, forces and torques in main parts of crane, and influence of load swinging. Diagrams will be presented for main parts of crane as the solution results of the analyzed system. Results gained will be used to get conclusions about dynamic behavior of crane, present graphs of main parameters and search for regulation of optimal jib rotation. Analysis will be done using modeling and simulations with computer application MapleSim. Also, results gained from simulations will be compared with those from experimental measurements.*

Keywords: TOWER CRANE, CRANE'S JIB, SCHEMATIC DESIGN, DYNAMIC ANALYSIS, ROTATIONAL MOTION, SYSTEMS REGULATION, MODELING, SIMULATIONS

1. Introduction

Tower crane taken for analysis is tower crane, the type of construction cranes with horizontal jib attached to the mast. Model of tower Crane is designed with software MapleSim 6.1 [3]. It is created based on data from manufacturer *Wolff* (Fig.1), [1]. Technical data for the model of crane are: Length of Jib: $L_j = 44$ *m*, Mass of Jib: $m_j = 5230$ *kg* $= 51.3$ *kN*; Mass of counterweight jib: $m_{lj} = 2000$ *kg* $= 19.62$ *kN*; Counterweight mass: $m_{co} = 8000$ *kg* $= 78.48$ *kN*; Height of Mast: $L_{ms} = 28.7$ m, Height of upper mast: $L_{ums} = 4$ *m*, Mass of mast: $m_a = 27310$ *kg* $= 268$ *kN*; Max carrying load: $Q_{max} = 62$ *kN*; Jib angular velocity: $\omega = 3.5$ *deg/s*. (Fig.2)

Fig. 1. Crane type Wolff 6531.6, at the place of work [1]

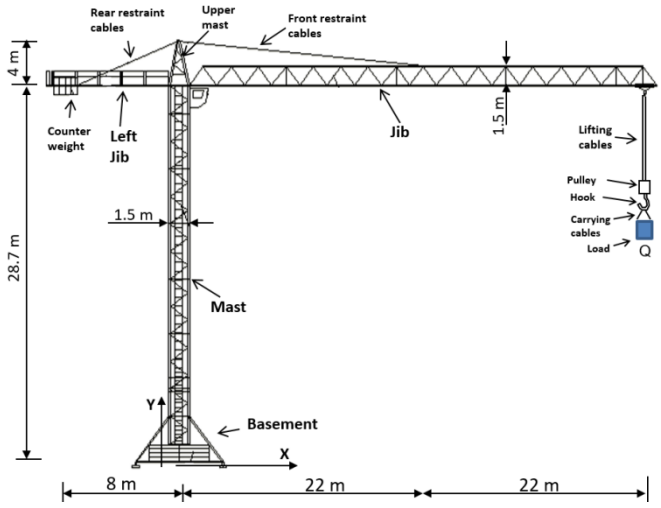

Fig.2. Tower crane main parts and dimensions [1]

Study is based in the theory of crane dynamics, multibody dynamics and systems design. It is a contribution to the topics of cranes: dynamic analysis, Modeling & Simulation of construction cranes, control and optimization of rotational motion, Sustainable design and control, Safety of heavy lifting devices.

2. Schematic design of Tower crane

In Fig. 3 is presented schematic design and block diagram of tower crane created with software *MapleSim 6.1*, which enables topological representation and interconnects related components [3]. Schematic diagram is created in order to apply analysis, generate differential equations and apply simulations. Elements of diagram are chosen to best represent parts of crane and its motion through simulations.

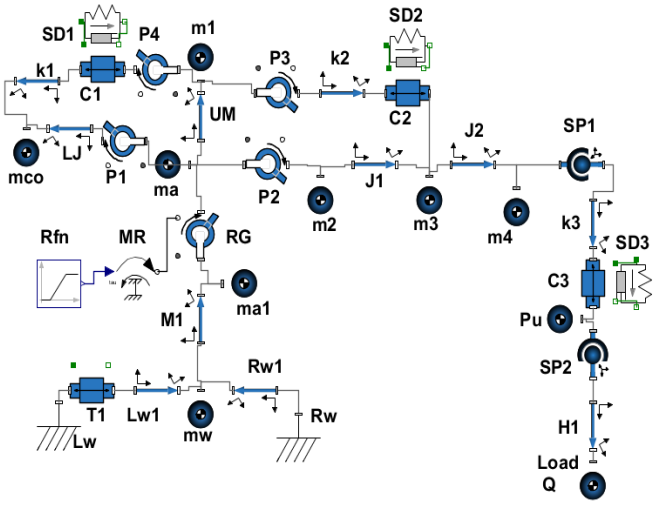

Fig. 3. Block Diagram of tower crane with jib rotational motion

Block diagram starts from left, with basement and mast of crane, and continues to the right where hoisting and Load Q is connected. All crane parts are designed with these elements (Fig.3):

- ***Rigid body frames*** **(bars):** Basement frames, left and right – *Lw1 & Rw1;* Mast- *M1;* Upper Mast- *UM;* Counterweight Jib- *LJ*; Jib first part- *J1*; Jib second part- *J2;*

- ***Fixed Frames*** – Left basement restraint - *Lw;* Right basement restraint – *Rw.*

- ***Concentrated masses:*** Basement mass – *mw;* Mass of mast – *ma, ma1;* Mass of upper mast- *m1*, Counterweight mass - *mco*; Masses of Jib-*m2, m3, m4;* Mass of Pulley system – *Pu*; Load - *Q;*

- ***Revolute joints***: Rotation Gear - RG; Rotation links - *P1, P2, P3, P4; Spherical links:* Link between jib and telpher – *SP1*; Hook link with pulley system – *SP2*.

On the Rotation Gear - RG is attached rotation motor *MR*, the element that gives the power - torque necessary to rotate the crane with angular velocity $\omega = 3.5$ *deg/s*. For best simulation scenario is implemented ramp function connected to rotation motor – Rfn.

- ***Restrain cables*** - are created with spring and dumping elements *SD1 & SD2*, translation link – C1 & C2, cable length – k1 & k2. Left side restraint cables elements – *k1, C1, SD1*; Right side restraint cables elements – *k2, C2, SD2*; Spring constant for restraint cables is $k = 500$ *kN/m* and Damping constant is $d = 7$ *kNm/s* [11].

- ***Lifting cables*** - are created with Spring and dumping element *SD3*, translation link – *C3*, cable length – *k3*; For the element SD1, pring constant for lifting cables is $k = 400$ *kN/m* and Damping constant is $d = 7$ *kNm/s* [11].

- ***Carrying cables*** – created with cable length element - *H1*.

Elements *SP1, SD3, C3, k3, Pu, H1 and Q* represents hoisting mechanism, and are modelled as double pendulum system. [2],[12]

In Fig. 3 is presented discrete-continuous model of crane used for model view and simulation. This model is 3-D visualization created by software recurring from Block diagram in Fig. 3. On this model, simulations will be performed in time frame of $0 < t < 20$ s. During this simulation time, crane will rotate 50º.

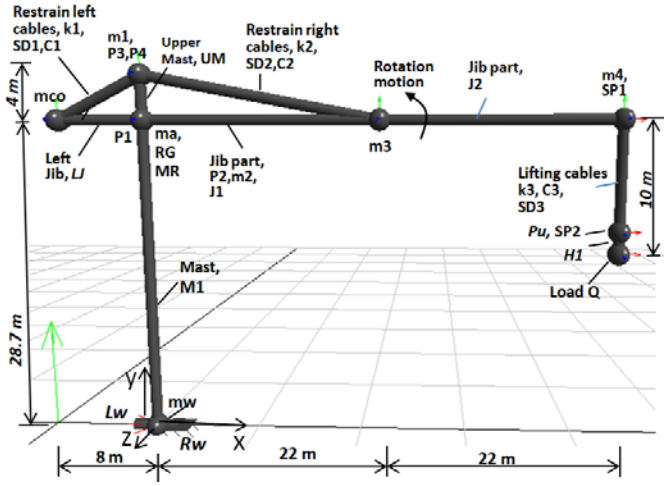

Fig. 4. Discrete-continuous model of tower crane in the form of 3-D visualization

3. *Differential equations of tower crane for the case of rotational motion*

To formulate dynamics of this system, standard Euler-Lagrange methods are applied, by considering the crane as a multi-body system composed by links and joints. For a controlled system with several degrees of freedom (DOF), the Euler-Lagrange equations are given as [7], [4], [8]:

$$\frac{d}{dt}\left(\frac{\partial E_k}{\partial \dot{q}_i}\right) + \frac{\partial E_p}{\partial q_i} = Q_i \qquad (i=1, 2...n) \qquad (3.1)$$

Where: q_i - are generalized coordinates for system with n degrees of freedom, E_k is Kinetic Energy, E_p is Potential energy, Q is the n-vector of external forces acting at joints. Kinetic energy for mechanical systems is in the form*:*

$$\mathrm{E_k}\,(q, \dot{q}) = \frac{1}{2}\dot{q}^T \cdot M(q) \cdot \dot{q} \qquad (3.2)$$

$\mathrm{E_p}(q)$ – is potential energy that is a function of systems position.

M(q) - is a symmetric and positive matrix of inertias [6].

Modern software's calculate physical modeled systems through mathematical models, numeric methods and Finite Elements Method. These calculations are based on Euler-Lagrange Equation (3.1), and forces acting on crane applied for regulation [5]. The modeling result is an *n*-degree-of-freedom crane model whose position is described by generalized coordinates $\mathbf{q} = [q_1 \ldots q_1]^T$, and which is enforced, in addition to the applied forces, by *m* actuator forces/moments $\mathbf{u} = [u_1 \ldots u_m]^T$, where m<n, [7]. The crane dynamic equations can be written in the following second order differential equation:

$$M(q)\cdot \ddot{q} + C(q, \dot{q})\cdot\dot{q} + \frac{\partial E_p}{\partial q} = Q(q, \dot{q}) - B^T\cdot u \qquad (3.3)$$

where **M** is the ***n x n*** generalized mass matrix, $C(q, \dot{q})$ is ***n x n*** matrix of Corriolis Forces, $\frac{\partial E_p}{\partial q}$ is the vector of gravity, **Q** is *n*-vector of generalized applied forces, and $\mathbf{B^T}$ is the ***n x m*** matrix of influence of control inputs **u** on the generalized actuating force vector $\mathbf{f_u} = -\mathbf{B}^T\mathbf{u}$, [7].

After completion and testing of model, Software Maplesim has powerful module for symbolic generation of differential equations. There are 18 DOF from crane model (Fig. 3), which gives 18 differential equations. Variables in differential equations are:

C1_F(t) – force in translational joint *C1*; ***C1_F2(t)*** – force 2 in translational joint *C1 (towards y)*; ***C2_F(t)*** – force in translational joint *C2*; ***C2_F2(t)*** – force 2 in translational joint *C2 (towards y)*; ***C3_F(t)*** – force in *C3* translational joint; ***C3_s(t)*** – motion in C3 translational joint; ***Pu_η (t), Pu_ξ(t), Pu_ζ(t)*** – variables of pulley mass Pu; ***Q_η (t), Q_ξ(t), Q_ζ(t)*** – variables of load Q; ***RG_M(t)*** – variable of moment-torque in the RG rotation Gear; ***P1_θ(t)–*** Rotational variable of P1 revolute joint; ***P2_θ(t)–*** Rotational variable of P2 revolute joint; ***RG_ ζ(t)–*** Rotation of revolute joint (rotation gear) RG; ***SD2 _s_rel(t)*** – Relative length of right restraint cables SD2; ***SD1 _s_rel(t)*** – Relative length of left restraint cables SD2.

3.1. Differential equations

There are 18 Differential equations that represents rotation motion of crane. They are long; we will present them in short form:

$$-4\cdot\sin(P1(\theta(t))) = 0 \qquad ...(3.1.1)$$

$$4\cdot\sin(P1(\theta(t))) = 0 \qquad ...(3.1.2)$$

$$-4+4\cdot\cos(P2(\theta(t))) - SD2\_s\_rel(t) = 0 \qquad ...(3.1.3)$$

$$4 - SD1\_s\_rel(t) - 4\cdot\cos(P1(\theta(t))) = 0 \qquad ...(3.1.4)$$

$$-C3\_F(t) - 400000\cdot C3\_s(t) - 7000\cdot\left(\frac{d}{dt}C3\_s(t)\right) = 0 \qquad ...(3.1.5)$$

$$576000\cdot\sin(P1(\theta(t)))\cdot\left(\frac{d}{dt}RG\_\theta(t)\right)^2\cdot\cos(P1(\theta(t))) - 4\cdot\sin(P1(\theta(t)))\cdot C1\_F(t) + 4\cdot\cos(P1(\theta(t)))\cdot C1\_F2(t) + \frac{5760000001}{10000}\cdot\frac{d}{dt}\left(\frac{d}{dt}P1(\theta(t))\right) - 706320\cdot\cos(P1(\theta(t))) = 0 \qquad ...(3.1.6)$$

$$-292180\cdot\cos(RG\_\theta(t))\cdot\cos(P2\_\theta(t))\cdot\sin(Pu\_\xi(t))\cdot\sin(Pu\_\eta(t))\cdot\cos(Pu\_\zeta(t))\cdot\left(\frac{d}{dt}Pu\_\xi(t)\right)^2\cdot C3\_s(t) + 1112320\cdot\cos(RG\_\theta(t))\cdot\cos(P2\_\theta(t))\cdot\ldots\cdot\cos(Q\_\xi(t))\cdot\left(\frac{d}{dt}\left(\frac{d}{dt}Q\_\zeta(t)\right)\right) - 291280\cdot\sin(RG\_\theta(t))\cdot\cos(P2\_\theta(t))\cdot\sin(Pu\_\xi(t))\cdot\cos(Pu\_\eta(t))\cdot\left(\frac{d}{dt}\left(\frac{d}{dt}C3\_s(t)\right)\right) + \frac{3}{5000}\cdot\frac{d}{dt}\left(\frac{d}{dt}RG\_\theta(t)\right) - RG\_M(t) = 0 \qquad ...(3.1.7)$$

$$-66200\cdot\cos(Pu\_\xi(t))^2\cdot\left(\frac{d}{dt}Pu\_\zeta(t)\right)^2\cdot\cos(Pu\_\theta(t))^2 + 6620\cdot\left(\frac{d}{dt}Pu\_\zeta(t)\right)^2\cdot C3\_s(t)\cdot\cos(Pu\_\theta(t))^2 + 6620\cdot\cos(Pu\_\xi(t))^2\cdot C3\_s(t)\cdot\left(\frac{d}{dt}Pu\_\eta(t)\right)^2 \ldots - 12640\cdot\sin(Q\_\eta(t))\cdot\sin(Q\_\xi(t))\cdot\sin(Q\_\zeta(t))\cdot\left(\frac{d}{dt}Q\_\xi(t)\right)^2\cdot\cdot\sin(Pu\_\xi(t))\cdot\sin(Pu\_\eta(t))\cdot\sin(Pu\_\zeta(t)) = 0 \qquad ...(3.1.8)$$

$$12640\cdot\sin(Pu\_\xi(t))\cdot\sin(Pu\_\eta(t))\cdot(\frac{d}{dt}Pu\_\xi(t))^2\cdot C3\_s(t)\cdot\cos(Pu\_\eta(t))\cdot\sin(Q\_\xi(t))\cdot\sin(Q\_\eta(t))+...+126400\cdot\cos(Q\_\zeta(t))\cdot\sin(Q\_\xi(t))\cdot\cos(Q\_\eta(t))\cdot\sin(Pu\_\xi(t))\cdot\cos(Pu\_\eta(t))\cdot\cos(Pu\_\zeta(t))\cdot\frac{d}{dt}(\frac{d}{dt}Pu\_\theta(t))+\frac{252800001}{10000}\cdot\frac{d}{dt}(\frac{d}{dt}Q\_\eta(t))=0 \quad ...(3.1.9)$$

$$-2912800\cdot\sin(RG\_\zeta(t))\cdot Sin(P2\_\theta(t))\cdot\cos(Pu\_\zeta(t))\cdot\cos(Pu\_\xi(t))\cdot\frac{d}{dt}(\frac{d}{dt}Pu\_\zeta(t))+...+582560\cdot\sin(RG\_\theta(t))\cdot\sin(P2\_\theta(t))\cdot\sin(Pu\_\xi(t))\cdot\sin(Pu\_\eta(t))\cdot\sin(Pu\_\zeta(t))\cdot\frac{d}{dt}(\frac{d}{dt}Pu\_\zeta(t))\cdot(\frac{d}{dt}C3\_s(t))=0 \quad ...(3.1.10)$$

$$132400\cdot C3\_s(t)\cdot\frac{d}{dt}(\frac{d}{dt}Pu\_\eta(t))+6620\cdot C3\_s(t)^2\cdot\frac{d}{dt}(\frac{d}{dt}Pu\_\eta(t))-662000\cdot\cos(Pu\_\xi(t))^2\cdot\frac{d}{dt}(\frac{d}{dt}Pu\_\eta(t))+126400\cdot\sin(Pu\_\zeta(t))\cdot\sin(Pu\_\xi(t))\cdot\cos(Pu\_\eta(t))\cdot\sin(Q\_\eta(t))\cdot\cos(Q\_\xi(t))\cdot\sin(Q\_\zeta(t))\cdot\frac{d}{dt}(\frac{d}{dt}Q\_\xi(t))=0 \quad ...(3.1.11)$$

… …. ….

$$\frac{d}{dt}SD1\_s\_rel(t)=\frac{-1}{7000}\cdot C1\_F(t)-\frac{500}{7}\cdot SD1\_s\_rel(t) \quad ...(3.1.17)$$

$$\frac{d}{dt}SD2\_s\_rel(t)=\frac{-1}{7000}\cdot C2\_F(t)-\frac{500}{7}\cdot SD2\_s\_rel(t) \quad ...(3.1.18)$$

4. Experimental measurements

Measurements in the tower crane are done in the place of work, where crane is mounted, in one local company in Prishtina, Kosovo (Fig.1 and Fig.5). They will be used for validation of results. Main measured parameter was force in carrying cables – *Fh (Fy)*. It was measured with dynamometer type *Dini Argeo* attached to the Hook [10], during the rotation of crane (Fig.5). There were 5 measurements achieved, and results are shown in Table.1:

Time (s)	Force in carrying cables - Fy (N)
1	61800
5	62600
8	63100
11	62350
17	62150

Table 1. Results of Fh (Fy) with dynamometer in carrying cables

Fig.5. Measurements with Dynamometer during rotation of crane

5. *Graphical results for main parts of crane*

Based on the model created, differential equations gained, and simulations, results are achieved for main dynamic parameters [2], [9]: *Velocity (v) (m/s), Acceleration (a) (m/s^2), Angular velocity (w) (rad/s), Angular acceleration (α) (rad/s^2), Force (F) (N), Force Moment-Torque (T) (Nm)*. Results are achieved after simulations are applied on designed system, Fig.3 & Fig.4. Simulations are planned to reflect real rotation of crane in order to achieve reliable results and comparable with experimental measurements. Time of simulation is t = 20 s.

Rotation motion is achieved with moment-torque generated ftom rotation motor MR, as a power element in the system (fig.3). It enables simulation of jib rotation. Simulation has three phases (Fig.6) [4],[9]:

First phase – Initial rotation. Value of power torque is M_t = 70000 Nm. Time of rotation is 0 s <t < 14 s. *Second phase* – Stopping phase of Jib rotation that usually lasts few seconds, while there is no sudden stop of motion in reality. This phase starts after first phase, and lasts 3 seconds, at simulation time 14 s <t < 17 s. *Third phase* – there is no torque from motor MR, value is M_t = 0. Jib rotation will slow down until it stops. It lasts between time 17 s < t < 20 s, which is the end of simulation. It is implemented in order to monitor end of rotation.

Simulation of crane rotation is achieved with adjustment of torque given from rotation motor RM, using ramp function *Rfn* **(**Fig.3, Fig.6). Regulation of rotation motion with regulation of torque is achieved through numerous tests in order to achieve planned simulation and angular velocity ω = 3.5 deg/s, and to get best results with less oscillations [2], [9], [4]. The value of torque gained from simulations that accurately represents rotation of jib is M_t = 70000 Nm = 70 kNm. This is the main process of regulation and control of crane rotation in this paper [5]. Other important parameters for regulation are:

- Hoisting mechanism - Spring and dumping element SD3 and translation link C3, in order to minimize effect of vibrations which appears in lifting cables and jib during rotation [7]. Spring constant for SD3 is determined with value *k = 400 kN/m* and damping constant is *d = 7 kNm/s* [11].

- Restrain cables - elements SD1, C1, SD2, C2. Spring constant for SD1 and SD2 is determined with value *k = 500 kN/m* and damping constant is *d = 7 kNm/s* [4]. Restraint cables have higher stiffness than lifting cables.

Next will be presented graphical results for main parts of crane, where horizontal axis is time (t = 0…20 s) and vertical axes are corresponding values of dynamic and kinematic parameters. Only most significant graphs will be shown.

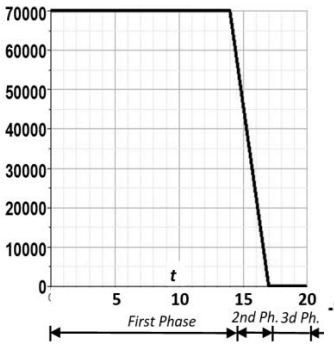

*Fig.6. Ramp function **Rfn** of torque M_t , (Nm)*

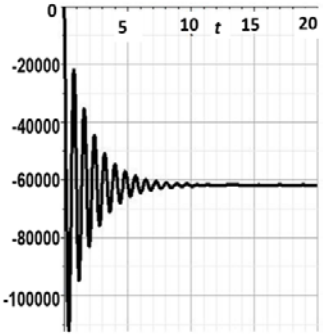

Fig.7. Force Fh (Fy) in carrying cables (ro1), (N)

5.1. Results for carrying cables H1 and Load Q

Carrying cables – *H1* (fig.3) and load *Q* are connected together as part of hoisting mechanism, and are being carried by crane's jib. Load *Q* makes swinging and oscillations during rotation motion. This behavior influences directly and indirectly other parts of tower crane. Results of main parameters are shown in Fig.7 to Fig.11. It is important to identify dynamic behavior of carried load in order to understand dynamic occurrences that affect other parts of crane.

In Fig.7 is graph of vertical force *Fy* in carrying cables *H1*. Force *F(y)* is Componential Force towards *y* axis, in negative direction. It has average value of $F(y) \approx |-61000|$ N, which is close to measurements in *Tab.1*. This validates results achieved with modelling and simulations. Values of other components *F(x)* or *F(z)* are small and will not be shown in graphs. In Fig.8 are shown acceleration *a(y)* and angular acceleration *α(x)* for carrying cables H1. Graph of acceleration *a(y)* in cables is more intense at the start of rotation. Graph of angular acceleration *α(x)* has heavy dynamic curve at entire process of rotation.

In Fig.9 are given graphs of load Q changing position in distance *x* and *y*, during rotation.

In Fig.10 are given velocity components *v(y)* and *v(z)*, which concludes that load *Q* has irregular motion and oscillations. *v(y)* is very intense at the start of motion, due to swinging of load toward y axes, but after time t≈10 s it has low oscillations. *v(z)* is velocity on *z* axes, that increases until t = 14 s, and after that it stops, due to decrease and stop of motor torque M_t (Fig6). *v(z)* has less oscillations than *v(x)*.

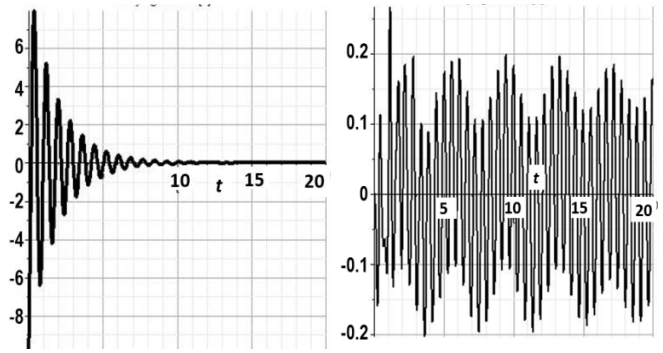

Fig.8. Carrying Cables H1 – acceleration a(y) (m/s^2) and angular acceleration α(x) (rad/s^2)

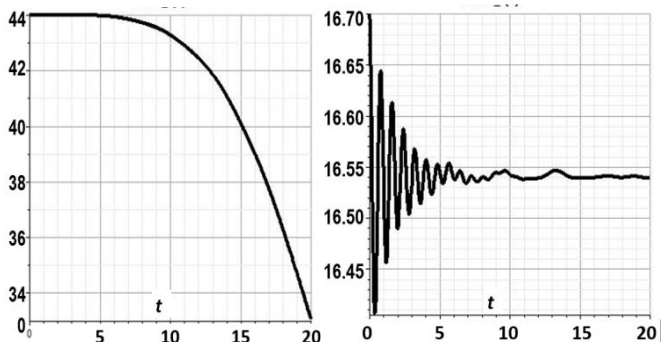

Fig.9. Position of Load Q – in x and y axes (m)

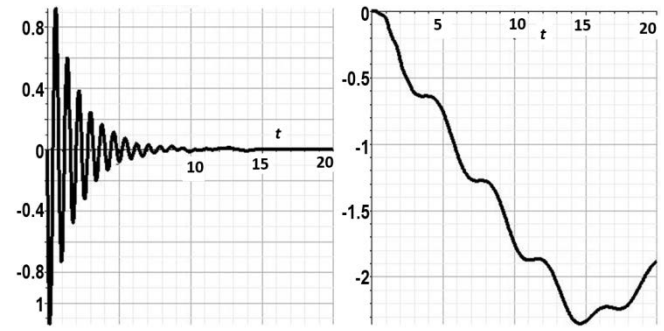

Fig.10. Load Q – Velocity v(y) and v(z), (m/s)

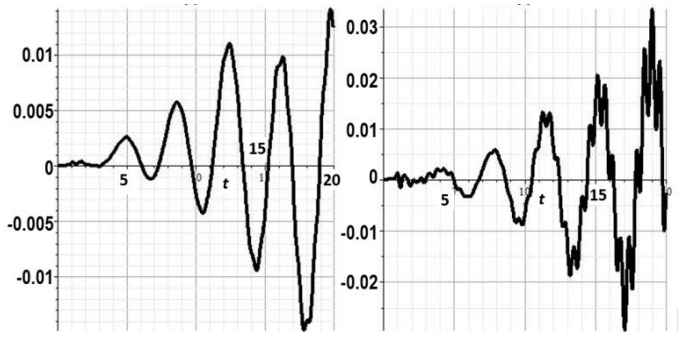

Fig.11. Load Q – angular velocity w(x) and angular accel. α(x)

In Fig.11 are given graphs of angular velocity *w(x)* and angular acceleration *α(x)* of load Q. Curve of these parameters is dynamic, in a form of sinusoids, with medium periods of oscillations and high amplitudes, which are intense after t > 5 s.

5.2. Results for Crane's Jib

Jib of tower crane is considered most important part for rotation motion (Fig.1 & Fig.2). It is a horizontal metallic structure with the grid of beams. Dynamics and oscillations from the load Q and hoisting mechanism are passed on the Jib. Results of main parameters – kinematic and dynamic for the Jib first part-*J1* are shown in Fig. 12 to Fig.15. Important conclusion is that oscillations occurring on Load *Q* and lifting cables are passed on the Jib of crane with similar form of curve, periods, and frequencies.

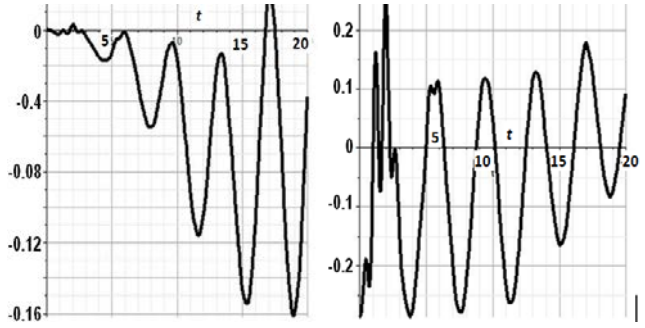

Fig. 12. Acceleration a(x) and a(z) in the Jib, (m/s^2)

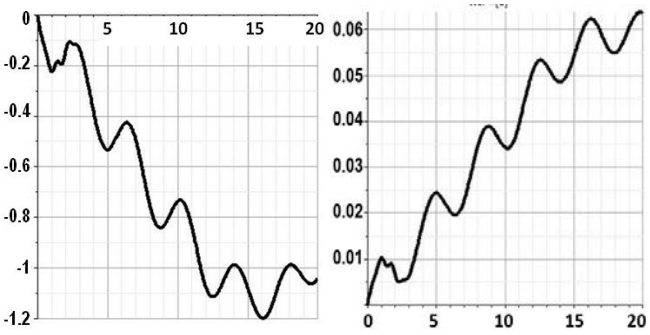

Fig. 13. Velocity v(z) (m/s), and Angular velocity w(y) (rad/s) in the Jib

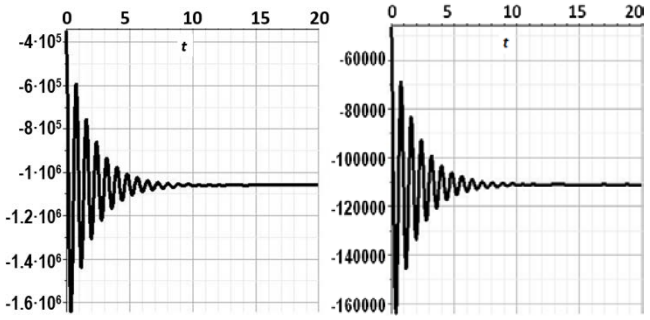

Fig. 14. Force components F(x) and F(y) in the Jib, (N)

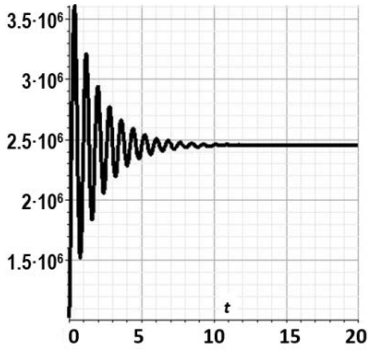

Fig. 15. Torque T(z) in the Jib (Nm)

Based on graphs and parameters taken for analysis, we can conclude that parameters are dynamic in nature, almost on entire process of Jib motion, with high oscillations and amplitudes at the start of rotation process.

5.3. Results for Restraint cables

Restraint cables (*k1* and *k2*) have stabilizing effect for crane's Jib and counterweight Jib. In fig.16 are given graphs of acceleration *a(x)* and angular acceleration *α(y)*. Conclusion is that these cables are under heavy dynamic process with high amplitudes.

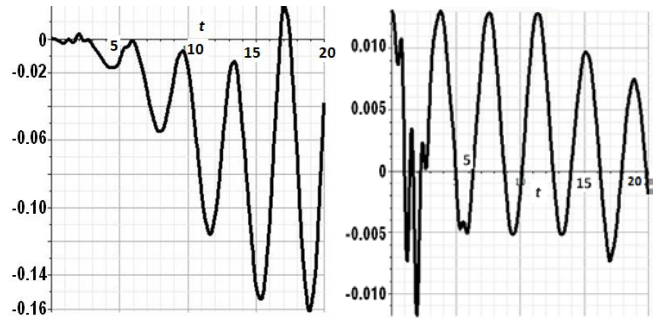

Fig. 16. Acceleration a(x) (m/s^2), and angular acceleration α(y) in Right restraint Cables, (1/s^2)

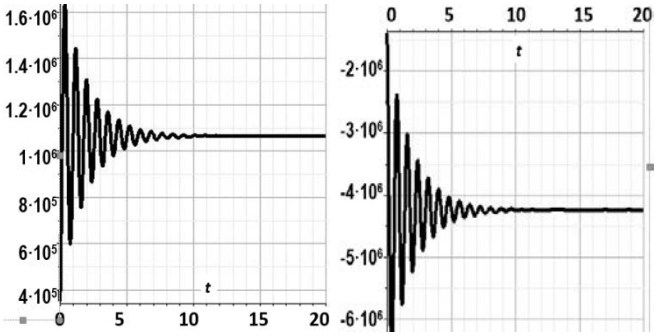

Fig. 17. Force F(x) (N), and torque T(z) (Nm), in Right restraint Cables

In fig. 17 are shown graphs of active force component F(x) and Torque *T(z)* that act on right restraint cables. At the beginning they undergo heavy oscillations, which after t>10 s decrease.

5.4. Results for Crane's Basement

Basement of crane is part where crane is mounted on the ground. In Fig. 2 is shown with two Fixed Frames named *Lw* and *Rw*, bars *Lw1* and *Rw1* and mass *mw*. Force component *R(y)* in Fig. 18 is reaction force. Graph has dynamic form of curve, with oscillations at the start of rotation. Max value of force F(y) is: F_{ymax} = |-570000| N, at the start of rotation process. After time t > 5.5 s, values are lower and less dynamic, with low oscillations. Values of *R(x)* and *R(z)* are small and not shown.

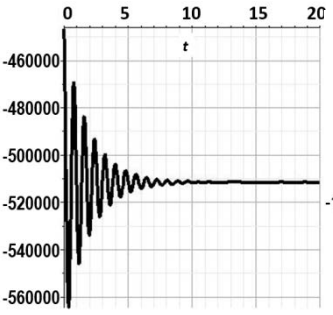

Fig.18. Force component R(y)

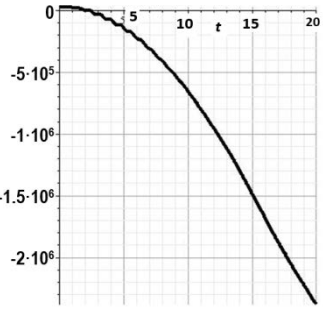

Fig.19. Torque T(x) (Nm)

In Fig.18 to Fig.21 are given graphs of components for moment-torque in the Basement. Oscillations from the Jib and Restraint cables are passed at the Basement, which most important support for keeping the stability of crane. In Fig. 20, value of torque is similar in form as initial torque given by the motor MR (Fig.6). Negative values of torques, and for other parameters in this work, are based on orientation towards referent coordinate system, originating in the Basement's center point (Fig.2, Fig.4).

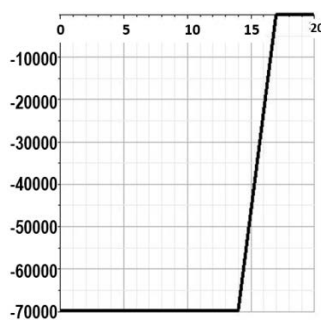

Fig.20. Basement - Torque T(y)

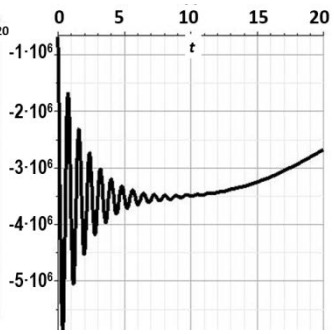

Fig.21. Basement - Torque T(z)

6. Conclusions

The main problem in tower cranes during rotation are oscillations as dynamic occurrences. It is important to identify and regulate them. Essential to the design of high performance motion control is the development of accurate mathematical models – in order to describe the crane dynamics [12]. To do this we created crane model with schematic design and 3-D visualization. Important part of analysis is creating accurate model and implementing proper simulations plan that reflects real crane's rotation motion, so that results are reliable. Results are gained for main dynamic parameters and compared with experimental measurements. From results it can be concluded that oscillations in all parts of crane are heavy and mostly with irregular occurrence. They occur in different planes. Oscillations have high intensity are mostly at the start of process. Minimizing oscillations was achieved through planning of rotation torque, parameters of hoisting mechanism, parameters of restraint cables and numerous simulations, in order to find optimal rotation [4], [8]. This is done with the aim to optimize the value of rotation torque in the motor which is important parameter for regulation and optimization. This work is also important for safety at work with cranes. It can be used also for further optimization analysis for other work processes like load lifting and telpher travel of tower crane.

7. References

[1] Construction crane manual, type Wolf 6531.6, Germany.

[2] Doçi I., Hamidi B., *Studying rotational motion of Luffing Jib Cranes with maximum load using simulations*, International Journal for science, technics and innovations for the industry-MTM 2015; 1(12): 20-24.

[3] *MapleSim User Guide*, Maplesoft, a division of Waterloo Maple Inc., 2014.

[4] Dresig, H., *Shwingungen mechanischer Antriebssysteme, Modellbildung, berechnung, analyse, synthese*, Springer Verlag, Berlin, 2001.

[5] S. Joe Qin, Badgwell Th.A., *An overview of industrial model predictive control technology*, Control Engineering Practice, A Journal of IFAC, ISSN: 0967-0661, 2003.

[6] La Hera, P. M., *Dynamics modeling of an electro-hydraulically-actuated system*, Umea University, 2011.

[7] Garcíaorden, J. Carlos, Goicolea, José M., Cuadrado Javier, *Multibody Dynamics, Computational methods and ap*plications, p.91, Springer, 2007.

[8] Vaughan J., *Dynamics and control of mobile cranes*, Georgia Institute of Technology, 2008.

[9] Doçi Ilir, Lajqi Naser, *Development of schematic design model of gantry crane for dynamic analysis and regulation of travel motion*, MTM Journal, Issue 6/2017, p.268.

[10] http://www.diniargeo.com/men/scales/weight-indicators.aspx

[11] http://www.engineeringtoolbox.com/wire-rope-strength-d_1518.html

[12] F. Ju a, Y.S. Choo a, F.S. Cui, *Dynamic response of tower crane induced by the pendulum motion of the payload*, International Journal of Solids and Structures 43 (2006) 376–389.